Article

Experimental Production of Excess Correlation across the Atlantic Ocean of Right Hemispheric Theta-Gamma Power between Subject Pairs Sharing Circumcerebral Rotating Magnetic Fields (Part I)

Mandy A. Scott, Nicolas Rouleau, Brendan S. Lehman, Lucas W. E. Tessaro, Lyndon M. Juden-Kelly, Kevin S. Saroka & Michael A. Persinger*

Neuroscience Research Group, Human Studies and Biomolecular Sciences Programs, Laurentian University, Sudbury, Ontario, Canada P3E 2C6

ABSTRACT

There have been multiple historical and cross-cultural reports of excess correlation of specific experiences between individuals separated by thousands of kilometers. Recently there have been experimental demonstrations of excess correlations between measurable cerebral events for small percentages of test subjects. More reliable effects can be elicited when electromagnetic fields and photons are involved. In this experiment completed during the summer of 2015, 5 pairs of volunteers separated by more than 6,000 km wore identical cerebral toroids through which patterns of phase shifting, 30 nT magnetic fields that diminished the local magnetic field in both loci by 1-5 nT were exposed to the sequences that produced excess correlation in chemiluminescent reactions and shifts in pH. Compared to the various baselines and control procedures enhanced power between the right hemispheres of pairs of participants occurred during the interval documented to produce excess correlation. Specific analyses indicated diminished coherence within the theta band only within the right temporal lobes of the pairs. Sequential block analyses revealed that the paired brains' responses to pulsed tones at 6.5 Hz occurred within the 30-40 Hz band over the caudal temporal lobes during the exposures to the effector field. Primary independent component analyses verified these patterns. During the 6.5 Hz tones there was a peak in the spectral power density (SPD) at that frequency over the right temporal lobe of the person listening but a trough in (SPD) over this region for the person who was not. Even subjective experiences, as measured by the Profile of Mood States (POMS), indicated significantly increased excess correlation for scales by which increased anger and decreased vigour are inferred. This experiment, based upon physical principles, suggests there is a technology that can generate reliable excess correlation of brain activity (and potentially consciousness and specific experiences) between two people separated by thousands of kilometers.

Part I of this two-part article includes: 1. Introduction; 2. Method; 3. Equipment; and 4. Results and Discussion.

Keywords: Excess correlations, entanglement, transatlantic effects, theta frequency, right temporal lobe, toroidal magnetic fields, brain coherence.

*Corresponding author: Dr. M. A. Persinger, mpersinger@laurentian.ca

1. Introduction

Consciousness has been strongly correlated with a single brain's structure and electromagnetic activity most typically measured by electroencephalography (EEG). The interaction between two loci associated with consciousness has assumed that distance is limited because locality is required. It is mediated by proximal physical stimuli such as visual or auditory events. However from an operational perspective as long as reliable, specific excess correlation for measureable events occurs between person A and person B, distance is not limited. Even from a classical behaviorist perspective the reciprocal interactions between two people are simply the manifestations of alternating stimulus-response sequences. We have developed a paradigm to evoke powerful excess correlations between chemilumiscent reactions (Dotta and Persinger, 2012; Dotta et al, 2013a) shifts in pH within spring water (Dotta et al, 2013b), and alterations in malignant cell growth (Karbowski et al, 2015) within two loci separated at distances between 10 m and 3 km. Here we present experimental evidence for the first known trans-Atlantic excess correlations in the type of brain activity associated with consciousness when the brains of pairs of people, each separated by thousands of kilometers, share toroidal, rotating magnetic fields with changing angular velocities.

The Nature of Locality and Causality

The definition of a causal relationship between a stimulus and response depends upon their space-time contiguity and whether or not the display of the responses systematically follows the occurrence of the stimuli. Examples are bright light flashes that elicit eye blinks or the verbal behavior of one person that elicits the verbal behavior of another. The usual perspective is: 1) there is some proximity between the locus of the stimulus and the locus of the response, and, 2) the correlation approaches 1 such that for every stimulus there is always a specified response. This would be an example of the maximum limit or "asymptote" for excess correlation which is often described as causality. However near thresholds or limens for perceptual phenomena such as detecting the presence or absence of a tone the elicitation of a response to a stimulus is not one-to-one but becomes a weaker and weaker correlation until there is some point where the "excess correlation" does not vary from random variation. As aptly demonstrated by decades of research in psychophysics signal detection around thresholds is a multivariate process where even chaotic distributions or stochastic components can enhance the capacity to discern the signal.

When the two loci that are attributed to the stimulus and response are separated by distances that do not appear to involve proximity or locality, the mechanisms for any excess correlation may be different. Dozens of theoretical approaches and experiments have shown that non-local effects are easily reproduced for quantum systems. The measurement involves photons (Vaziri, et al, 2002). Experimental free-space quantum teleportation involving photons has been measured at distances of up to 600 m according to Jin et al (2010). However Hotta et al (2014) has indicated that quantum energy teleportation does not necessarily display a limit of distance. Megidish et al (2013) showed that entanglement can occur between photons that never coexisted in traditional space-time, which suggests that specific modifications of the electromagnetic-gravitational features of spaces could induce excess correlation. This interpretation is consistent

with the theory developed by Hu and Wu (2006a, b; 2013) that the primary source of the macroscopic manifestation of quantum entanglement originates from primordial spin processes in non-spatial and non-temporal pre-space-time and involves gravity. When one considers the measurement by Fickler et al (2013) that single photons (even though they differ by 600 in quantum number as long as they exhibit quantized orbital angular momentum from helical wave structures) can exhibit excess correlation, then the potential for remote sensing become feasible.

Entanglement is defined as "when the quantum system contains more than one particle, the superposition principle gives rise to the phenomenon of entanglement" (Aczel, 2002). The superposition principle, or more specifically the principle of superposition of states, indicates that a new state of a system may be composed of two or more states such that a new state emerges that shares some of the properties of each of the composite states. If X and Y are two different properties of a particle, for example existing in two different loci, then superposition indicates a condition X+Y arises which has properties of both entities. Thus there would be a non-zero probability that the particle could be in both loci simultaneously. The application to a "multi-particle" system or one that involves more than one photon has been shown experimentally. Macroscopic manifestations of "excess correlation" have also been shown. Julsgaard et al (2001) demonstrated excess correlation in two macroscopic objects (gas molecules). Dotta and Persinger (2012) measured this effect with millions of photons each generated by separated reactions of hypochlorite and hydrogen peroxide.

Development of the Theory and the Technology

Excess correlation at spaces greater than quantum levels may appear to require physical conditions that allow the superposition of two loci such that they display the behavior of a single space. Based upon the conceptual approaches of Ernst Mach (1988), Sir Arthur Eddington (1981), Niehls Bohr (1958), and Hu and Wu (2006a, b; 2013), we had reasoned that the circular momentum of a quantized electromagnetic field could create the condition to facilitate entanglement between two loci (and the state of matter within those loci) separated by non-traditional distances (Persinger and Koren, 2013; 2014). The essential premise is that the physical mechanisms that serve as the substrate for entanglement reflect the properties of the entire universe as a unit within which differences in space and time may be less critical. It would be similar to Hu and Wu's (2013) concept that it is a feature of the universe before space and time emerged as properties with which they are now recognized.

Our initial methodology employed bursts of weak magnetic fields rotating within a circular array of 8 solenoids. The angular velocity of these rotating magnetic fields either increased or decreased. The pattern of the magnetic fields that were produced within each solenoid in the circular array of solenoids was produced by a computer program that generated pulsed or punctate 1 ms or 3 ms fields that composed either an accelerating or decelerating frequency-modulated and phase-modulated magnetic field. The durations of ~1 ms and ~3 ms were derived from our (Persinger and Koren, 2007) calculations that these two values reflected the time for an electron and a proton to expand one Planck's Length. Since those initial quantifications, several experimental results have supported this interpretation (Persinger, 2013a; Koren et al, 2014).

Inspired by the importance of the difference in phase and group velocities of photons in order to produce a non-zero rest mass (Tu et al, 2005) Dotta and Persinger (2012) compared the effects of different combinations of accelerating and decelerating group velocities (the changing angular velocities of the whole field rotating around the array of solenoids) and accelerating and decelerating frequency-modulation or phase-modulation of the patterns of magnetic fields that were being generated by the computer to each solenoid. The change in velocity was accomplished by adding +2 or -2 ms to the base duration of 20 ms as the field rotated around the ring of solenoids. They found that only one combination produced excess correlation. The group angular velocities were equivalent to frequencies between 5 and 20 Hz with specific locations around the array where the acceleration was convergent with g: 9.8 $m \cdot s^{-2}$.

If an initially accelerating group velocity embedded with a decelerating frequency-modulation field was presented first (**the primer field**), the subsequent presentation of a decelerating group velocity embedded with an accelerating frequency-modulated field (**the effector field**) produced excess correlation of photon emissions between two loci separated by either 10 m or 3 km for about 8 minutes. These were the only two distances tested. During the approximately 8 min interval the power density of the photons emitted from the chemical reactions in one location was double that of the typical measures. In fact it was equivalent to injecting twice the reactant into a single reaction when there was no excess correlation. This was consistent with our assumption that the structure of the two loci separated by non-traditional distances behaved as if they had been superimposed into a single space. In other words, the states exhibit superposition.

The Electroencephalogram and Brain Imaging

The most frequent tool employed to study consciousness is electroencephalographic activity. These measurements obtained from sensors located more or less equally over the surface of the scalp measure the variations in the averaged, distant electric fields from the approximately 20±5 billion neurons that compose the human cerebral cortices (Pakkenberg and Gundesen, 1997). We have employed the 10-20 international system. Although other researchers who prefer denser sensor arrays we have found this matrix is sufficient to discern the phenomena we are investigating. The measurements are within the microvolt range. The corresponding magnetic field component exhibits picoTesla values and is consistent with the product of magnetic permeability of a vacuum and the current density from these voltages within the resistivity of extracellular fluid across the length of the human brain (Persinger and Saroka, 2015; Saroka and Persinger, 2014).

Quantitative electroencephalography (QEEG) was a major development that permitted the quantized perspective to be applied to brain activity. The decomposition of fluctuations from scalp sensors into quantized microvolt increments markedly increased the complexity and numbers of measurements and permitted the consideration of QEEG activity as a field potentially composed of "infinite, infinitesimal points". When real-time brain activity from 19 sensors is sampled between 250 to 1000 times per second the density of the potential data arrays is sufficient to discern very subtle changes from the environment yet manageable for routine analyses. Such complexity could be sufficient to demonstrate the subtle changes in two locations

displayed by two human brains that could meet the criteria for "excess correlation" or entanglement.

QEEG has the potential to manifest excess correlation because the data can be considered as representative (or by inference) of a "state" composed of a more or less reliable field or pattern of frequencies and intensities. There are reliable microstates first described by Lehmann et al (1998) and standardized by Koenig et al (2001) that remain relatively consistent across a person's life time. There are primarily four states of whole cerebrum organization with polarities arranged in left frontal to right caudal, right frontal to left caudal, frontal to caudal and central frontal to caudal patterns. They accommodate more than 70% of cerebral activity. Each state exists for about 80 to 120 ms, the duration of a "percept," and is remarkably similar across human beings. The median value is conspicuously equivalent to 10 Hz.

The concept of a field involving billions of neurons would appear to contain considerable momentum that would oppose alteration by a single, small source energy. There is clear experimental evidence that very small energies can alter states composed of millions or billions of units. Houwelling and Brecht (2008) found that the activity of only one neuron could affect the direction of a rat's motor behaviour. Within a single barrel cortical column containing about 8,500 excitatory neurons, detection required 2,500 action potentials above the 1,500 action potentials (a difference of 1,000) per 200 ms period. This means that the initiatory detection and the whole-organism effect required only about 5 action potentials per 1 ms. Later Li et al (2009) reported that repetitive high frequency spiking of only a *single* rat cortical neuron could trigger a shift between two cortical states that resembled rapid-eye-movement (REM) and slow wave sleep.

In other words the energies required to produce significant alterations in brain states and overt behaviour are in the order of 10^{-20} J. This is the energy from the effect of the net change of an action potential upon a unit charge (Persinger, 2010). It is also a likely increment of energy that might integrate the distribution of energy at the level of Planck's Length throughout the universe. The total force within the universe based upon its mass, length and squared "Zitterbewegung" frequency divided by the total number of Planck's voxels in the universal volume distributed across the wavelength of the hydrogen line results in 10^{-20} J (Persinger, et al, 2008; Persinger, 2015). Thus very small increments of energy transmitted through non-local space could alter the entire pattern of global brain activity.

Previous Experiments of EEG-Related Excess Correlation

Hans Berger, the pioneer who developed the concept and original tools that now define modern electroencephalography, was interested in explaining a personal experience that would now be identified as a potential example of excess correlation between his exposure to a trauma that could have been deadly and the cerebral ideation of his sister who was living in different city of that country. The first major high profile experiment showing that two (2) of 15 pairs of twin infants separated by non-traditional distances displayed excess correlation in elicitation of alpha rhythms was published by Duane and Behrendt in *Science* in the year 1965. Although there were many interesting preliminary studies involved with "extrasensory perceptual" research, including that of a martial arts master who was instructed to emit "qi" force and the concurrent increase in

strip-chart alpha wave moving in a rostral direction from the occipital region of the student recipient sitting in another room (Kawano, et al, 2000), direct experimental manipulation of the process has been more rare.

Standish et al (2004) reviewed about a dozen experiments involving "remote transfer of signals" from the previous 40 years. Standish and her colleagues found that 5 of the 60 subjects displayed reliable visually evoked potentials when their "senders" were viewing flickering but not static light displays. In a previous experiment Standish et al (2003) had demonstrated excess correlation between the MRI signals of two brains separated by non-traditional distances. Although there have been many reports of specific or exceptional individuals who report "spontaneous" experiences consistent with excess correlations at greater distances (Dotta et al, 2009; Scott and Persinger, 2013), without experimental manipulation or simulation of these conditions within the laboratory, the mechanisms cannot be isolated. In addition both the Duane and Behrendt (1965) and Standish et al (2004) experiments indicated that the effects were not demonstrable in all pairs of "senders" and "receivers". The relative portion is in the order of about 10%.

We have assumed that the spontaneous occurrences of excess correlations between the activities of two different brains separated by non-traditional distances suggest an aggregate phenomenon within which one component is essential. The analogy would be the remarkable analgesic and antipyretic effects of white willow bark. The clinical effects were often variable. However when late 19th century methods for organic chemistry were developed that allowed the extraction and later synthetic reproduction of the specific component (acetyl salicylic acid) that was responsible for the analgesia and antipyresis, the effects could be more reliably replicated between individuals. We have assumed spontaneous excess correlations between human brains separated by thousands of kilometers are natural phenomena that, like the white willow bark's correlation with analgesia, can be reliably elicited once the critical variables are isolated and experimentally manipulated.

Persinger et al (2003) first reported that the stimulation of one of a pair of siblings with a circular array of 8 solenoids placed around the head at the level of the temporal lobes produced a specific change in theta power (5 to 5.9 Hz) in the right temporal lobe of the other sibling (not wearing an array of field-generating solenoids) sitting blindfolded with earplugs in a separate room. The rates of rotation of the magnetic that were most effective involved 20 ms reference intervals. Additions or subtractions of unit times, such as 2 ms, as the field moved to each successive solenoid produced a changing angular velocity. This interval which is more likely a range between 15 and 25 ms is the classic "refresh" rate of consciousness (~40 Hz) which has been described as the rate of "re-entry" of continuous processes (Edelman, 1989). It can be considered a second derivative. A magnetic field moving within a circle might be considered as in a state of continuous acceleration. Changing that rate would result in a second derivative.

Because one of the features of excess correlation or entanglement is a history of shared space-time, Persinger et al (2008) paid pairs of random strangers to meet each other for one hour twice per week for four weeks and simply remain within a meter of each other. When one of the pair who had been randomly assigned to the entanglement process was stimulated with the same effective field parameters (20 ms intervals) while wearing the circular array of 8 solenoids and

the other member's QEEG was recorded there was an increase in power within the 5.0 to 5.9 Hz band over the temporal lobes but no other lobes. Pairs of people randomly selected on the days of the experiment who had no previous shared space-time history did not display this effect.

In that experiment the stimulus person (the one receiving the angular accelerating magnetic fields) was instructed to imagine walking to the other room and standing on the left side of the response person whose QEEG was being recorded. The response persons, during the period associated with the enhanced theta activity over the temporal lobes, reported (as indicated by post-experimental questionnaire responses) an increased incidence of sensed presences, anger, and sexual arousal. These effects were not reported by the other members of the pair who were exposed to the rotating magnetic fields or by the response persons who composed the random pairs of subjects for the reference (control) group.

These studies were predicated on the concept that the magnetic field condition for one person was a type of stimulus while the response in the EEG for the other person (no field) was the consequence of this effect. Subsequent experiments, which were similar to the excess correlation experiments for photon-chemical reactions (Dotta and Persinger, 2012) and shifts in pH (Dotta et al, 2014), involved both loci or the brains of both participants in a pair being exposed to the same rotating magnetic fields around each of their heads. The demonstration of proof of principle involved a reliable shift in the intercorrelations of QEEG sensor data over the scalp for the "receiver" person sitting blind folded and wearing ear plugs in one room while the "stimulus" person sitting in a closed, acoustic chamber was exposed to a series of different frequency lights (Persinger et al, 2010). The changes in the intercorrelations in the response person's brain when the stimulus person's brain was being exposed to the light flashes occurred over the *right* posterior hemisphere.

Dotta et al (2011) extended this study by measuring the photon emissions from the right hemisphere of the response person who was sitting in complete darkness while wearing one of the circular arrays of solenoids. When the stimulus person (also wearing the array of solenoids, was sitting in a closed acoustic chamber) was stimulated with light flashes the response person's right hemisphere displayed an increase in photon flux density when measured at a distance of about 15 cm. The reversible increases and decreases of these ultraweak biophoton emissions from one person as a function of the light exposure to a second (stimulus) person in another room was within the range of 10^{-11} to 10^{-12} $W \cdot m^{-2}$. This effect only occurred if both the stimulus and response persons were wearing the solenoid arrays and were simultaneously exposed to rotational fields with changing angular velocities. The results suggested that when both loci, or both person A and B, were exposed to the specific parameter of circular rotating weak (microTesla) magnetic fields with changing angular velocities changes consistent with excess correlation were stronger and more likely to occur reliably.

Estimated Magnitude of Energies

Any mechanism that is involved with excess correlations between two brain loci separated by non-local distances should involve energies that reflect those that involve the processes that mediate the effect. Saroka and Persinger (2014) and Persinger and Saroka (2015) have shown that the basic frequency and the harmonics of the Schumann Resonance (7-8 Hz, 14

Hz, 20-21, 26-27, 33-34, 39-40 Hz, etc) can be discerned within the spectral profiles of most human brain activity. Most all terrestrial organisms are immersed in these fields or their variants. The manifestation of the Schumann Resonances and the harmonics are more evident within the caudal portions of cerebral activity than more rostrally.

The magnitudes of both the electric field and the magnetic field of human cerebral electroencephalographic activity are similar to those of the fundamental Schumann resonance. These values are in the range of mV per meter for the electric field and 1 to 2 picoTesla for the magnetic field. The Schumann resonance is primarily generated by global lightning strikes whose average incidence is about 44±5 Hz (Christian, et al, 2003) which is the median interval of the gamma frequency frequently associated with consciousness. The propagating field from a single lightning discharge returns to the source over the spherical guide in about 20 to 25 ms with a phase shift of 13 ms within this 7 to 9 Hz interval. As shown by Llinas and his colleagues (e. g., 1993) the recurrent 20 to 25 ms propagating waves that integrate large areas of the human cerebral cortices occurs between the rostral and caudal cerebrum. This particular pattern occurs predominately during waking and dream sleep but not during slow wave sleep. The phase modulation is about 12.5 ms.

Even from a conservative electrophysiological perspective brain tissue displays a resonance frequency with a medium value in the 7 to 8 Hz range. According to traditional empirical measurements the permeability (inductance, L, per meter) of cortical grey matter at frequencies around 1 kHz is about 10^{-2} Henrys. This frequency (1 kHz) is equivalent to 1 ms which is the effective duration of the action potential of most neurons. The energy of a single action potential with this duration produced by the product of the shift in voltage and the unit charge is about 10^{-20} J which reflects both the magnitude and duration required to stack a base nucleotide upon the type of RNA sequence the produces the proteins that some neuroscientists consider the substrate of memory (Persinger, 2010). The permittivity value, C (capacitance), for grey matter is $2 \cdot 10^{-1}$ $F \cdot m^{-1}$. Application of the classic formula:

$$f=[\sqrt{2\pi \cdot (LC)^{-1/2}}]^{-1} \quad (1),$$

results in about 7 Hz.

The immersion of human brains within an electromagnetic pattern that shares peak spectral frequencies and electric and magnetic field intensities produces the condition for a pervasive diffusivity. The resistivity of the whole brain's primary constituent (physiological water) is about 2 $\Omega \cdot m$. When multiplied by magnetic susceptibility ($4\pi \cdot 10^{-7}$ $N \cdot A^{-2}$) the resulting diffusivity is $1.7 \cdot 10^{6}$ $m^2 \cdot s^{-1}$. The median potential difference for QEEG activity per Hz is ~$2 \cdot 10^{-6}$ V (2 μV). When this value is divided by $1.7 \cdot 10^{6}$ m^2 s^{-1} the equivalent magnetic field strength is about 10^{-12} T (pT). This is the value of the magnetic component of the Schumann Resonances. The convergence does not prove a variable that produces diffusivity is necessary for the similar strength magnetic field. However it suggests that a fundamental feature of space, magnetic permeability, with the exact conditions (extracellular fluid conductivity) within which a collection of neurons (a brain) interact could produce a conduit for this global interaction.

The functional duration for all human brains immersed within a common medium to be potentially interconnected has been calculated to occur within about 8 to 9 min (Dotta and Persinger, 2012). Assuming the conductivity of physiological saline within each brain to be σ=0.5 $S \cdot m^{-1}$, the magnetic diffusivity would be $0.63 \cdot 10^{6}$ $m^2 \cdot s^{-1}$. If the surface area of each human cerebrum is assumed to be $\sim\pi \cdot 10^{2}$ m^2 the total surface area for 7 billion human brains would be $22 \cdot 10^{7}$ m^2. When this value is divided by the magnetic diffusivity term the resulting value is 349 s or about 6 min (Persinger, 2013b). One interpretation is that if there was some factor that simultaneously integrated or "connected" all brains because they shared the same medium, such as the earth's static magnetic field within which the Schumann patterns are embedded, then the time required for a change in one brain to affect any one or all of the other 7 billion brains would be about 6 min.

This latency does not reveal the quantity of the effect being mediated. If $\sim 10^{-20}$ J is associated with the excess correlation as a basic unit about 10^{7} neurons each discharging around 10 Hz would be required to achieve the threshold for a percept where the person might be aware of the effect (Rouleau and Dotta, 2014). However if the demonstration by Houwelling and Brecht (2008) is applied and this magnitude of energy is sufficient to affect the overt response of an animal, an effect could occur without necessarily the awareness or perception of the effect. The phenomenon of "blind sight", for example, involves adaptive responses during ambulation of technically blind people. fMRI data indicate that small numbers of occipital cortical neurons respond to the optic stimuli but the numbers are not sufficient to meet the threshold at which "conscious awareness" occurs.

The conditions for the two similarities, from a signaling perspective, could be consistent with Lorentz's Lemma which relates any two electromagnetic fields if: a) they are the same frequency, b) outside of the source, and c) in a linear isotropic medium. If we assume: 1) the two fields are the Schumann resonance generated between the surface of the earth and ionosphere by lightning and the cerebral resonance generated between the corona of the cortices and the multiform layer of the cerebrum by action potentials (Persinger, 2012), and, 2) the Schumann Resonance and cortical fields are harmonic in time, then:

$$\text{del} \cdot (\mathbf{E}_b \times \mathbf{H}_s) = \text{del} \cdot (\mathbf{E}_s \times \mathbf{H}_b) \quad (1),$$

where **E** refers to the electric field vector component, **H** is the magnetic field ($A \cdot m^{-1}$) vector component and the subscripts refer to b (brain) and s (Schumann) sources. The aggregate is Watts per meter squared. For both the human and the Schumann Resonances, this value is $\sim 10^{-12}$ $W \cdot m^{-2}$. This is also the power density emitted from the right hemisphere of subjects imagining white light while sitting in a hyper-dark environment (Dotta and Persinger, 2011; Dotta et al, 2012).

As predicted by the Lorentz Lemma, Persinger and Saroka (2015) demonstrated *real time* intermittent coherence between the spectral power within the Schumann frequencies associated with the brain activity of 41 men and women and ionosphere measures. Transient coherence of spectral power densities with the first three modes (7-8 Hz, 13-14 Hz, 19-20 Hz) of the Schumann Resonance in real time were measured from local (measured in Sudbury) and distal (measured in Italy) stations. The duration of the coherence was for about 300 ms about twice per

min. This suggested that the "interface" interval between the global Schumann field within the spherical wave guide and each brain was once every ~30 s.

Topographical map clusters indicated the domain of maximum coherence was within the *right* caudal hemisphere within the volume occupied by the parahippocampal gyrus. These clusters, associated with shifts of about 2 μV, became stable about 35 to 45 ms after the onset of the synchronizing event. During the first 10 to 20 ms the isoelectric lines shifted from clockwise to counterclockwise rotation. Persinger and Saroka (2015) concluded that the results were consistent with the congruence of the frequency, magnetic field intensity, voltage gradient, and phase shifts that are shared by the human brain and the earth-ionospheric spherical wave guide. The observation that the intermittent coherence for brain measures was similar for measurements of the Schumann values in Italy and within a few meters (locally) of where the brain activity was being measured suggested that coherence might occur *any where on the planet* for some individuals. This capacity might be considered a major antecedent variable for phenomena represented as "non-local".

There are multiple examples of measurements demonstrating the magnetic fields of the cognitive correlates of brain function and of the Schumann Resonance at the fundamental (7-8 Hz) are about 10^{-12} T and the electric field components are about 1 $\mu V \cdot m^{-1}$ to 1 $mV \cdot m^{-1}$. The Lorentz Lemma adds the dimension of radiant flux density. For the human brain with an average of 1 μV per 10 cm per Hz or 10^{-5} $V \cdot m^{-1}$ and current gradient of $1 \cdot 10^{-6}$ V divided 2 Ω·m or $0.5 \cdot 10^{-6}$ $A \cdot m^{-1}$, the flux power density would be about $5 \cdot 10^{-12}$ $W \cdot m^{-2}$. This is the same order of magnitude as the photon flux density emitted from the earth and during human cognitions associated with imagination and thinking of white light when sitting in hyperdark settings (Dotta et al, 2012). The involvement of photons within a "macro-entanglement process" is expected from both theory and measurement because quantum phenomena manifested as discrete shifts of change in energy between electron shells is considered the bases of "entanglement". A similar concept, employing a different perspective, has been developed by the extraordinary original thinker Pitkanen (2012; 2013; 2014).

The Present Experiment

The major limit of our DAC (Digital-to-Analogue Convertors) technology is that is not readily accessible to the population. We (St-Pierre and Persinger, 2006) have found that when a technology is too complex its application by others (Persinger and Koren 2005) is often erroneous because of the numbers of requirements for function. This leads to results that can be misinterpreted. What was required was equipment that: 1) could be easily constructed by the average person and 2) imitated or replicated the excess correlation effects we have found in the laboratory. Burke et al (2013) found that when a toroid was placed over the head (level of the temporal lobes) of each individual in a pair separated by about 400 km while each subject's QEEG was being measured, LORETA profiles indicated excess correlation in the activity within the temporal lobes of both subjects when one of the pair was exposed to sound patterns. The effect was not observed with visual stimuli.

The excess correlation also occurred *only* during the component of the experiment when the rotating magnetic fields were functioning in a decelerating manner that simulated the

conditions in which double photon emissions were measured by Dotta and Persinger (2012). However in the Burke et al (2013) experiments the fields were generated from the programs within laptop computers to Arduino circuits that could be easily constructed. This meant that there was the potential for any person to construct the equipment with readily available components to replicate and extend this research.

Rouleau et al (2014) employed the same double toroid and Ardueno system within which two containers of spring water were placed in order to verify that the arrangement produced the excess correlation in the pH shift that was reported for the DAC system by Dotta et al (2013b). Rouleau and his colleagues (2014) found that the excess correlation effect was discernable within the component of the presentation of the field that was most similar to the "entanglement" phase of the DAC studies. In addition Rouleau and Persinger (2015) later found that the intensity required to produce the effect associated with the activation of these counterclockwise, experimental rotating fields (0.3 mG) was a small decrease in intensity of the ambient geomagnetic field between 1 and 5 nT. This small diminishment occurred primarily in **the east-west direction** or within the direction of the axial rotation of the earth**.**

This small shift of 1 to 5 nT is not trivial. The change in magnetic energy for a shift of 5 nT within a cerebral volume of 10^{-3} m^3 would be about 10^{-14} J, or, the mass equivalent of an electron. The convergence with the energy-mass relationship for an electron could be considered essential given the intricate connections between quantum photon emissions and absorptions and electron shells. In addition, the product of 1 to $5 \cdot 10^{-9}$ $kg \cdot A^{-1} \cdot s^{-2}$ (T) and the rotational velocity ($\sim 4.5 \cdot 10^{2}$ $m \cdot s^{-1}$) at the latitudes in which our experiments were completed is in the order of 10^{-6} $V \cdot m^{-1}$. In other words a potential difference that occurs in the cerebral cortical fields of the human brain is coupled to the angular velocity of the earth itself for the same magnetic field intensities that characterize both the dynamic activity associated with the Schumann and human brain harmonics.

The present experiment was designed to discern if excess correlation between pairs of two brains separated by the Atlantic Ocean would occur specifically during the effector component of the paired toroid design. In order to integrate all of the major themes and procedures that have been involved with previous experiments that pursued excess correlations over long distances without the participation of traditional senses, the design involved multiple operations for different types of cognitions, such as eyes open or closed, imagining sending or imaging receiving light, listening to either pulsed (6.5 Hz) or continuous tones, and field on or field off conditions.

We appreciated that the demonstration for excess correlation between brain activities of two individuals separated by thousands of kilometers but who shared the "entanglement" magnetic fields would be embedded within the normal activity of the brain that reflected the behavioural contingencies and cognitive structuring of the experiment. These conditions were employed as reference points or comparator functions so that the effect size and strength of any evidence of excess correlation could be quantified. We also realized that an elegant, simple design would appeal to parsimony. However if consciousness is a complex, emergent phenomenon, then the opportunity for interactions of processes to occur was considered preferable. This required a more multivariate design.

2. Method

Participants

The participants (N=10) were 4 female and 6 male adults aged 23 to 57 years (mean age=33.5 years). During the experiment they were located in Sudbury, Ontario, Canada; Berlin, Germany; and Madrid, Spain. They were divided into Groups A and B and then paired by trial (e.g. A1 with B1, see Table 1). Group A (n=5, 3 female, 2 male, mean age= 30.4 yr) was the first to be cued to "send" while simultaneously Group B (n=5, 1 female, 4 male, mean age= 36.6 yr) was the first to be cued to "receive" white light, the active engagement conditions. Group A was also the first to receive the burst tone while Group B was first exposed to the single tone + silence, the passive engagement and "rest" conditions.

Table 1. Designation of Participants in the TransAtlantic Entanglement Experiments

	Group A				**Group B**			
Pair	**ID**	**Sex**	**Age**	**Location**	**ID**	**Sex**	**Age**	**Location**
1	A1	1	31	Sudbury	B1	1	39	Berlin
2	A2	1	30	Sudbury	B2	2	40	Berlin
3	A3	2	24	Sudbury	B3	2	57	Madrid
5	A5	2	42	Berlin	B5	2	23	Sudbury
6	A6	1	25	Berlin	B6	2	24	Sudbury

Procedure: TransAtlantic Entanglement

Each pair of participants from Groups A and B completed a single trial of the paradigm in June 2015 between 16:00 to 19:00 UTC. Timing was precise (within 1 s) in order to facilitate synchronous measurements at distances exceeding 6000 km. At agreed upon times based on UTC, experimenters in the NRG Consciousness Research Laboratory located in Canada coordinated with out-bound experimenters located in Berlin, Germany and Madrid, Spain to complete the TransAtlantic measurements of Non-Local Entanglement. The orientation (facing) of the pairs (A and B, respectively) were: N-N, E-E, S-E, N-SE, and N-NW.

The participants completed a demographics questionnaire and pre-test profile of mood states (POMS-SF) after which the experimenters applied the 19 channel (Mitsar EEG-201) quantitative electroencephalogram (QEEG) for continuous measurement during the 42 minute paradigm, as well as the toroid systems for the field application, to each participant in the pairing. Stop watches for pairs of Group A and B measures were synchronized by the experimenters (to the second) via video-teleconferencing (Skype). Once watches were synchronized and a start time was determined (~5 min from synchronization), communication between experimenters was ended and the participants were each read verbatim a script describing cuing instructions for the paradigm (see Appendix A). The participants were informed that the entire experiment, except for baseline measures, would be completed with eyes closed, and that verbal cues to send-receive would be followed by rest conditions cued by audible tones.

Table 2. Flow diagram of the temporal components of QEEG data extracted for analyses and the operations within each component.

#	1	2	3	4	5	6	7	8	9	10	11
Condition	EO-pre	EC-pre	Rest	S-R	R-S	Rest	S-R	R-S	Rest	S-R	R-S
Field	No field					Primer Field				Effector Field (I)	

#	12	13	14	15	16	17	18	19	20	21	22
Condition	Rest	S-R	R-S	Rest	S-R	R-S	Rest	S-R	R-S	EC-post	EO-post
Field			Effector Field (II)				No Field				

The experiment began with a 6 min baseline (3 min eyes opened then 3 min eyes closed) followed by a 1 min "rest" period, the onset of which was signaled by an audio cue (either burst tone or single tone + silence, for Groups A and B respectively). The carrier tone was 220 Hz while the pulsation of that tone was 6.5 Hz. Next Group A was cued to "send" while simultaneously Group B was cued to "receive" (condition S-R) for a duration of 2 min, after which the pairs switched (Group A receives while Group B sends, condition R-S) for another 2 min. Following this first block of send/receive conditions, the second 1 min "rest" period was cued and Group A received the single tone + silence while Group B receives the burst tone. The conditions alternated for a set of 6 send/receive + rest repetitions.

The magnetic field application was initiated through the Toroid + Arduino system at the start of the second rest period, 11 min into the paradigm, following one full trial of both passive and active engagement conditions (Rest, S-R, R-S), for a total duration of 20 min, involving 2 different magnetic field patterns. The second trial of entanglement conditions was completed during exposure to the first pattern, a counter-clockwise decelerating magnetic field pattern (minutes 11 to 17, for 6 min total).

At the end of the third rest period (min 17) the second field pattern was initiated. It was a counter-clockwise accelerating magnetic field. Send/Receive trials 3-5 were completed during the accelerating field exposure, from minute 17 to 31 in the full paradigm and minutes 6 to 20 within the magnetic field exposure time. The fields were turned off at the start of the 6^{th} and final rest period, at minute 31. The participants completed trial 6 of the send/receive paradigm post-field exposure before completing a 6 min post-experimental baseline measure (3 min eyes closed and 3 min eyes open). The participants completed the POMS (Profile of Mood States) before the beginning and at the end of the 22 sequences (42 min).

Table 3. Locations of the pairs of subjects and the estimated distances of separation.

City	Longitude	Latitude	UTC	Distance (km) to Sudbury
Sudbury, Canada	46.49° N	81.01° W	UTC-5	0
Berlin, Germany	52.52° N	13.38° E	UTC+1	6341
Madrid, Spain	40.40° N	3.68° E	UTC+1	6019

Quantitative EEG Data

The continuous data, spanning a total of 2520 sec, from each of the 19 channels for each of the pairs were extracted from WINEEG Software and imported into MATLAB for synchronization by pair. This allowed for artifact removal from paired data without compromising the synchrony of the measurements. The continuous synchronized data were then segmented into the 22 conditions (Table 2), from pre to post baseline. Segmented data were then spectral analyzed into 8 band ranges from delta to gamma (1.5-4.5, 4.5-7.5, 7.5-10, 10-13, 13-20, 20-25, 25-30, 30-44 Hz) and imported into SPSS Windows for further analyses. The segmented data were also entered into a series of coherence analyses within MATLAB comparing 19 x 19 channels within each pair, from A1 to B1, etc., across the 8 frequency bins.

3. Equipment

Toroid & Arduino

The devices consisted of identical torus-shaped coils coupled to identical microcontrollers receiving synchronized signal-generating procedures from separate laptop computers. Previous studies have shown that this configuration induced a stimulus-response pattern in human participants such that quantitative electroencephalographic (QEEG) activity associated with stimuli presented to an individual at location A was effectively displayed for a second, stimulus-naïve individual at location B where the paired participants were separated by over 300 km (Burke et al., 2013). Additionally, discrete pH shifts were recorded in coupled beakers of spring water such that the injection of a proton donor at location A (decrease in pH) was associated with reliable increases in pH (more alkaline) at location B where the paired beakers were separated by 1 meter (Rouleau, Carniello, & Persinger, 2014).

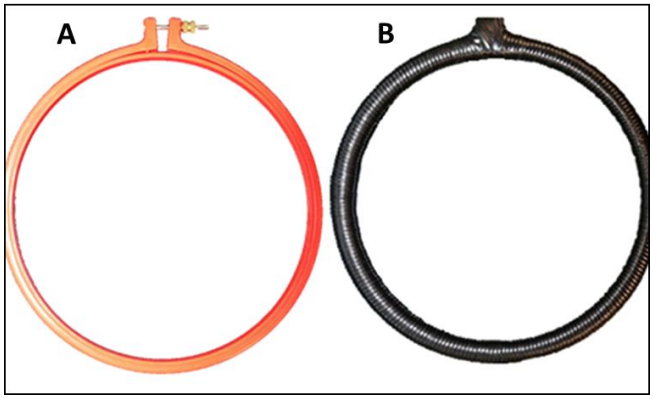

Figure 1. A plastic crotchet ring (A) before and after (B) copper wrapping. The coil is covered in black vinyl electrical tape.

Each coil consisted of a plastic ring with a diameter of 25.4 cm, wrapped in a single layer of 16 gauge insulated copper wire for a total of 225 turns around the 79.8 cm circumference (Figure 1). This toroid, fastened to the head by an elastic cap, was plugged into a solderless

breadboard equipped with the basic circuit seen in Figure 2. The details, including schematic representation, were specified by Rouleau & Persinger (2015).

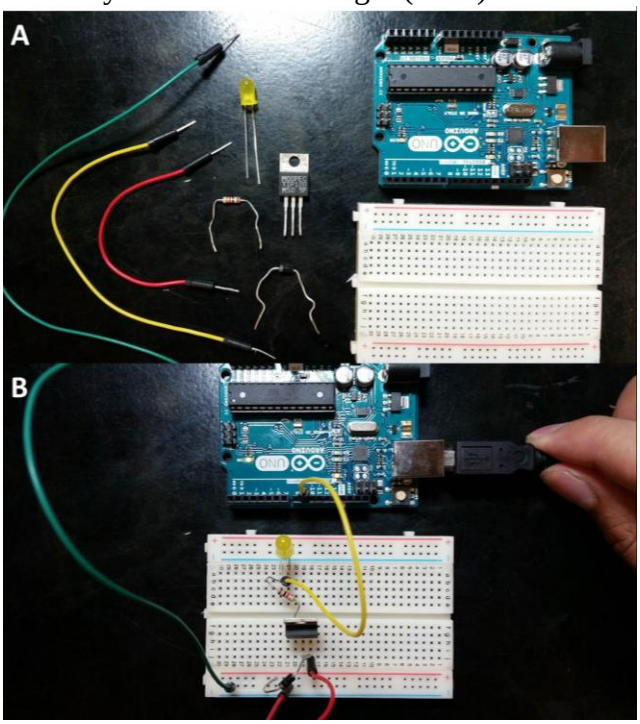

Figure 2. Components of the circuit disassembled (A) and assembled (B).

The solderless breadboard and coupled coil received pulsed current from an Arduino Uno R3 Microcontroller (as seen in Figure 2). Two pulse patterns were coded within the Arduino 1.0.6 software interface. The **Primer** pattern consisted of 7 all-or-none 3 ms point potentials which continuously looped, separated by incrementally longer inter-stimulus intervals beginning with 20 ms and increasing by 2 ms for every pulse, recycling back to 20 ms after the 7-pulse sequence. The 3 ms point duration was selected on the bases of calculations by Persinger and Koren (2007), derived from the Hubble parameter, for the time required for a proton to expand one Planck's Length. The **Effector** pattern involved the same all-or-none potentials. However, the inter-stimulus intervals between points starting with 20 ms decreased by 2 ms for every pulse. The code is partially displayed in Figure 3 whereas 2D representations of the pulse patterns are provided in Figure 4.

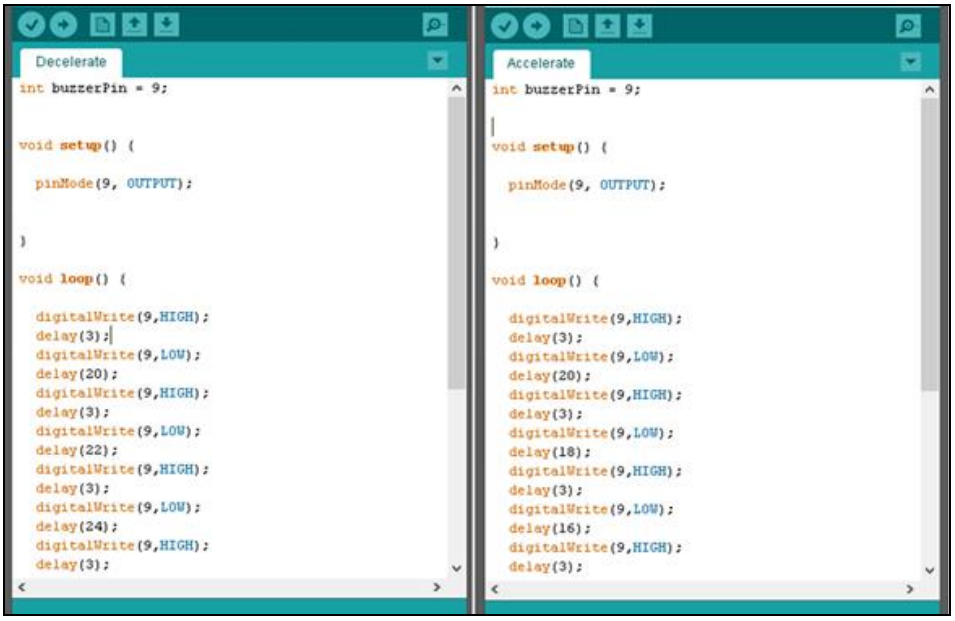

Figure 3. Arduino code for the Primer (left) and Effector (right) pulse patterns.

Once the fields were initiated, the duration of the whole exposure procedure was 20 minutes. The first field (Primer) was presented for 360 s and immediately followed by the second field (Effector), which was presented for 840 s. Rouleau and Persinger (2015) have reported that the electromagnetic fields generated within the center of the coils outputting these pulse patterns undergo 1-5 nT diminishments within the East-West horizontal axis referenced to Magnetic North as recorded by a MEDA FVM-400 Vector Magnetometer. A power frequency unit indicated that the strength of the pulsed magnetic fields rotating around the toroids averaged 30 nT (0.3 mG). This was the intensity that produced the largest excess correlation in the pH studies that employed this equipment.

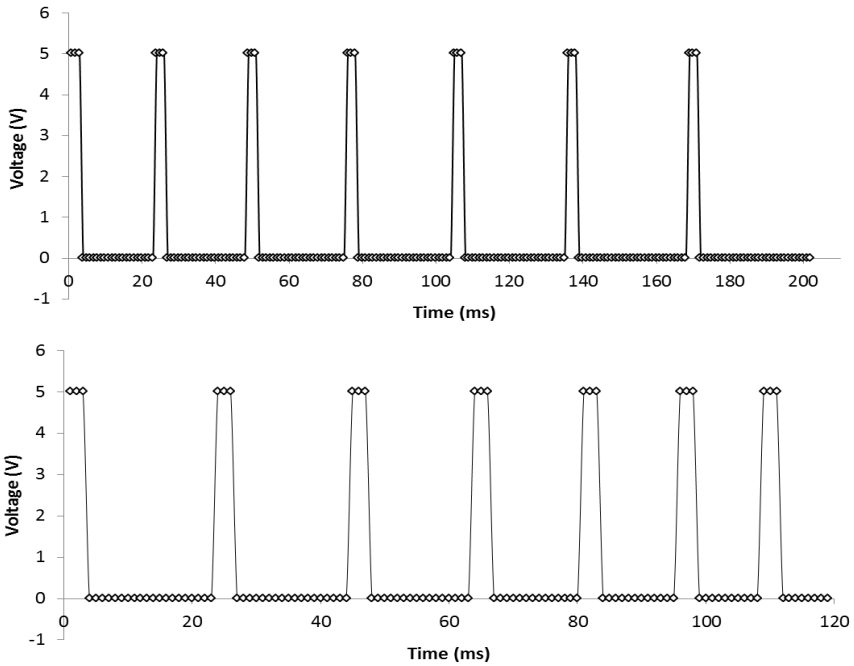

Figure 4. Primer (top) and Effector (bottom) pulse patterns as specified by the code. Each diamond represents a 1 ms point. Note that each pulse duration was 3 ms.

The field exposure procedure subsequent to cap application and antecedent psychometric data collection can be summarized succinctly. First, the participant was fitted with the toroid over the head (Figure 5). The participant then sat still in a comfortable chair while baseline QEEG recordings were obtained. The Primer pattern was initiated upon the 11th minute of the trial by plugging in the USB cord which connected the laptop to the microcontroller. Synchronization of this step across both locations was accomplished by strict adherence to pre-synchronized time keeping devices and the experimental schedules that accompanied them. Once connected by the USB cord, the microcontroller, breadboard, and coil drew power from the laptop. After 360 s had elapsed, the Effector pattern was initiated manually using the Arduino 1.0.6 software. Once uploaded, the Effector pattern cycled for 840 s. The field was terminated by unplugging the USB cord, thereby removing the power source of the device. QEEG recording continued until the 42nd minute of the experiment had elapsed.

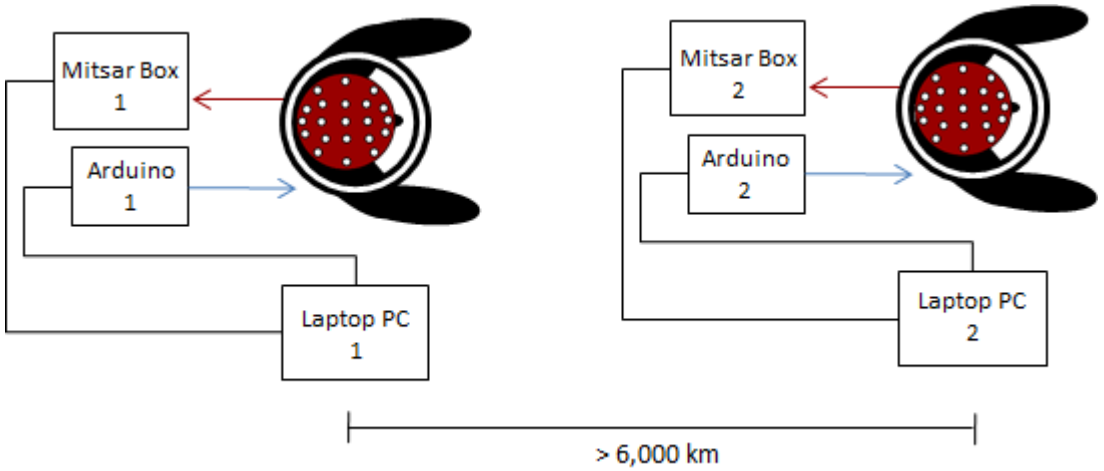

Figure 5. Schematic of the experimental equipment.

4. Results and Discussion

Expected Activities of Local Behaviours (Within Subject Brain Correlations)

In order to compare any statistically significant effects for the shared hemispheric correlations between subject (non-local) effects we measured the magnitude of intercorrelations between hemispheres **within** subjects, i.e., within the same brain. Table 4 shows the global power in µV for each person's left and right hemisphere as well as the net difference in power and the equivalent voltage when the eyes were opened. There were baseline differences in the two Mitsar boxes employed in the experiments. This is shown by yellow and grey color. However the net differences in voltage between the persons' left and right hemisphere were comparable for the two instruments.

Table 4. Global Power for the Left and Right Hemispheres of the 10 participants during eyes open conditions as well as the net difference in power and equivalent in microVolts. Yellow vs grey reflects the intrinsic characteristics of the two Mitsar devices.

			Eyes Open Global Power Converted to µV
Left Global Power	Right Global Power	Net Difference in Power	Net Difference in µV
49.22	50.58	1.36	7.236
24.57	23.44	1.13	6.595
19.8	21.95	2.15	9.098
25.55	28.53	2.98	10.711
30.53	37.44	6.91	16.310
8.64	6.9	1.74	8.184
4.44	4.6	0.16	2.481
3.07	3.32	0.25	3.102
12.28	8.48	3.8	12.095

6.49	8.29	1.8	8.324

Table 5 also shows the global power differences and net changes when the subject's eyes were closed. The net increase in μV global power when the eyes were closed was typical for the normal person and representative of what we have measured in the last approximately 500 subjects assessed with this technology. A separate analyses by another one of the authors showed that the average increase in global spectral power was about 5 to 10 μV higher during phases 2 through 21 of the experiment when the subjects' eyes were closed compared to the pre (phase 1) and post (phase 22) baselines whose average was 20 and 16 μV respectively.

Table 5. Global power for the left and right hemispheres for all 10 participants during the eyes closed conditions as well as the net differences in power between the hemispheres in microVolts. Yellow vs grey indicates the two Mitsar devices.

Eyes Closed Global Power Converted to μV			
Left Global Power	Right Global Power	Net Difference in Power	Net Difference in μV
5.6	6.05	0.45	4.162
5.51	4.31	1.2	6.797
3.22	3.69	0.47	4.253
11.44	8.96	2.48	9.771
7.36	7.17	0.19	2.704
38.62	40.6	1.98	8.730
50.7	44.26	6.44	15.741
29.28	34.97	5.69	14.800
36.31	41.66	5.35	14.351
81.42	99.65	18.23	26.493

The interhemispheric correlations for each subject across the phases of the experiment are shown in Figure 6. Because these measures reflected the intrasubject correlation of activity across hemispheres the expected near 1.00 values were expected. The coefficients for the 10 subjects per phase ranged between r=0.97 to r=0.99. From a neurofunctional perspective, the inter-correlations between the individuals' own lobes is significant. As seen in Figures 7 thorugh 10 the individual lobes are strongly intercorrelated. Although T3 (left) and T4 (right) sensors were least correlated and accommodated only 77% of the shared variance compared to the other examples (> 90% of shared variance), the effect is not statistically significant because of the sample size (n=10).

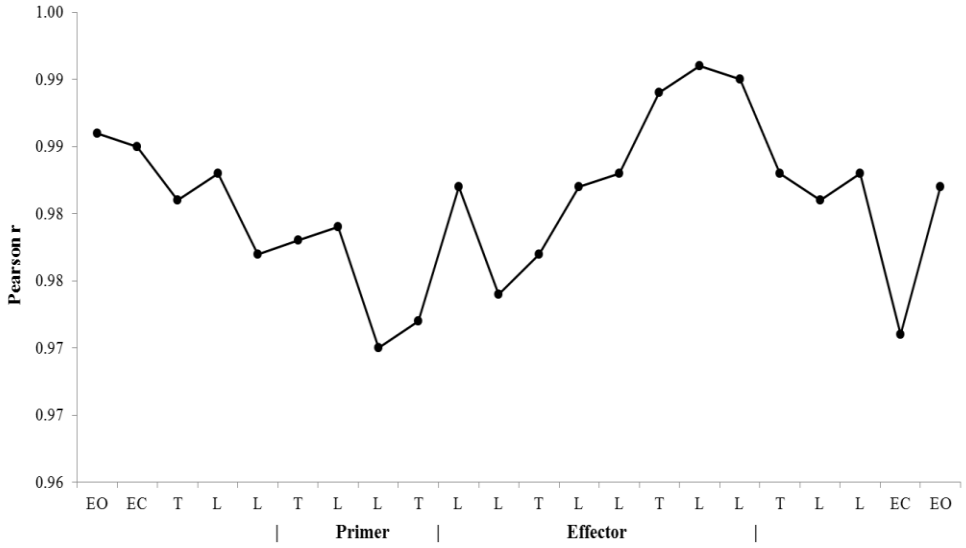

Figure 6. Within subject correlation between the magnitudes of the global power within the left and right hemisphere of the same brain for the 10 participants

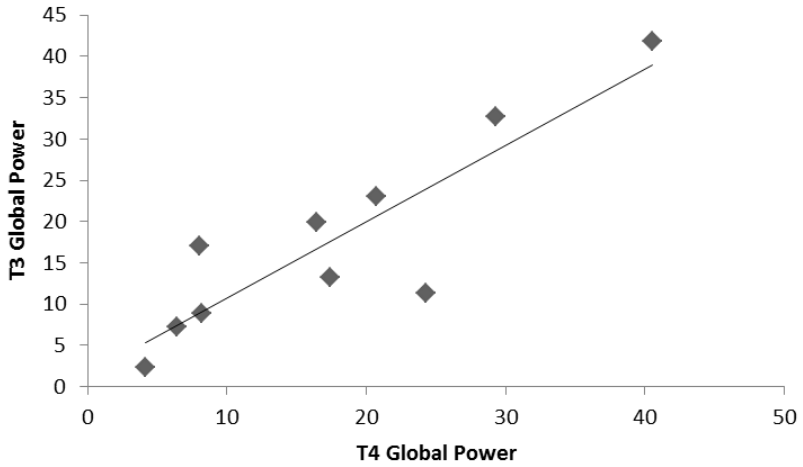

Figure 7. Correlation (r=0.88) between T3 and T4 global power for each person's brain (n=10) during eyes opened conditions.

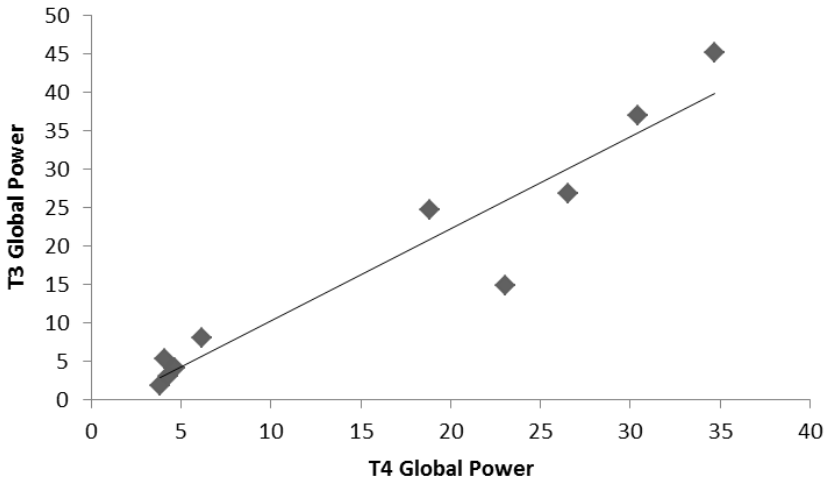

Figure 8. Correlation (r=0.95) between T3 and T4 global power for each person's brain (n=10) during eyes closed conditions

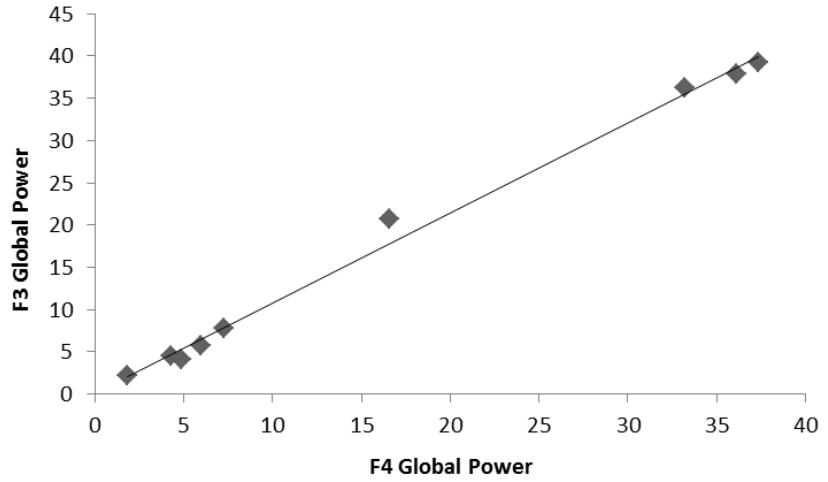

Figure 9. Correlation (r=0.99) between global power between the left and right frontal sensors for each person's brain during eyes closed condition.

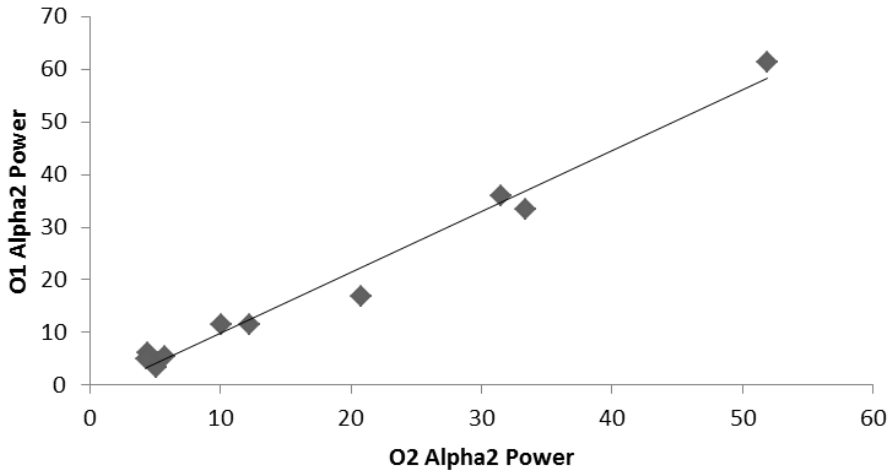

Figure 10. Correlation (0.99) between global power between the left and right occipital sensors within each person's brain during eyes closed condition.

*Excess Correlation Patterns **Between** Subjects at a Distance: Global Power*

The same methods of comparisons were completed for correlations of global power values between each pairs left hemisphere and right hemisphere even though they were separated by more than 6,000 km. During the Effector field sequence of the EMF exposure, statistically significant increased coherence of global spectral power density across **right** hemispheric sensors equivalent to a correlation coefficient of .88 could be discerned, explaining approximately 77% of the variance (Figure 11).

Spectral power densities were highly correlated over F4 ($r = .95$, $p<.05$; rho= .90, $p<.05$) and T4 ($r = .97$, $p<.01$; rho= .90, $p<.05$), which were the sensors located over the *right* frontal and *right* anterior temporal areas. Removing pairs systematically from the analysis revealed that a cluster of significant non-parametric correlation coefficients could be identified for right hemispheric global power during the second half of the Effector field sequence, continuing somewhat after the termination of the field ($p<.05$).

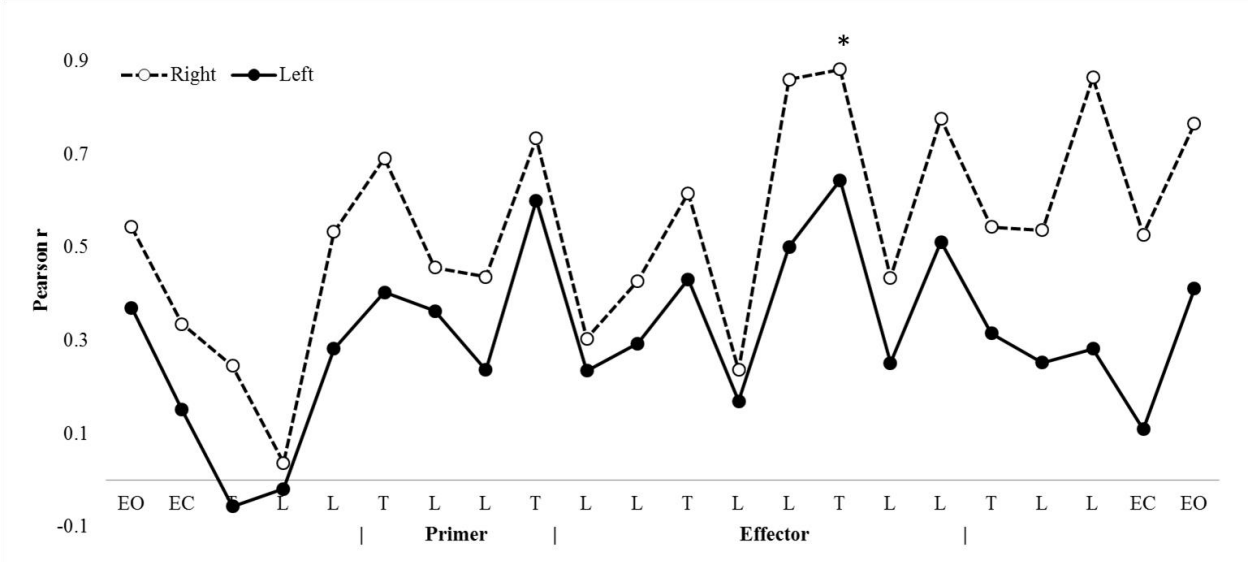

Figure 11. Correlation coefficients plotted overtime indicative of the strength of the association between paired right (light circle; dotted line) and paired left (dark circle; full line) hemispheric global spectral power densities. EO indicates baseline with eyes open, EC indicates baseline with eyes closed, L indicates white light visualization, and T indicates paired tone presentations.

Correlation coefficients presented in Figure 12 were loaded and chunked into 5 experimental sequences across time: Pre-Baseline (n=5), Primer (n=4), Effector 1 (n=4), Effector 2 (n=4), and Post-Baseline (n=5). An ANOVA revealed that correlation coefficients indicative of the strength of the association between global spectral power density over right hemispheric sensors of paired participants differed as a function of sequence, $F(4,21)= 3.83$, $p<.05$, $\eta^2= .47$. Left sensors did not demonstrate the effect after Bonferroni correction ($p<.05$). *Post-hoc* analyses revealed two homogenous subsets where the primary source of variance was accommodated by differences in the correlation coefficients during Effector 2 (M= .74, SE= .10) relative to Pre-Baseline (M= .34, SE= .09), $t(7)= 2.84$, $p<.05$, $r^2= .53$.

During the second half of the Effector field sequence (Effector 2), correlation coefficients indicative of the strength of the association between global spectral power density measures across QEEG channels for paired participants differed as a function of channel, $F(7,31)= 21.90$, $p<.001$, $\eta^2=.86$. As visualized in Figure 13, the weak association between paired right occipital sensors (O2) relative to all other sensor pairs was the major source of variance ($p<.001$). However, it should be noted that further differences among the remaining sensors were identified. Increased average correlation coefficients were noted for paired T6 sensors (M= .90, SE= .04) relative to paired C4 sensors (M= .74, SE= .05, $t(6)= 2.51$, $p<.05$, $r^2= .51$). Similarly, correlation coefficients were increased for paired F4 sensors (M= .92, SE= .03) relative to paired C4 sensors, $t(6)= 3.21$, $p<.05$, $r^2=.63$.

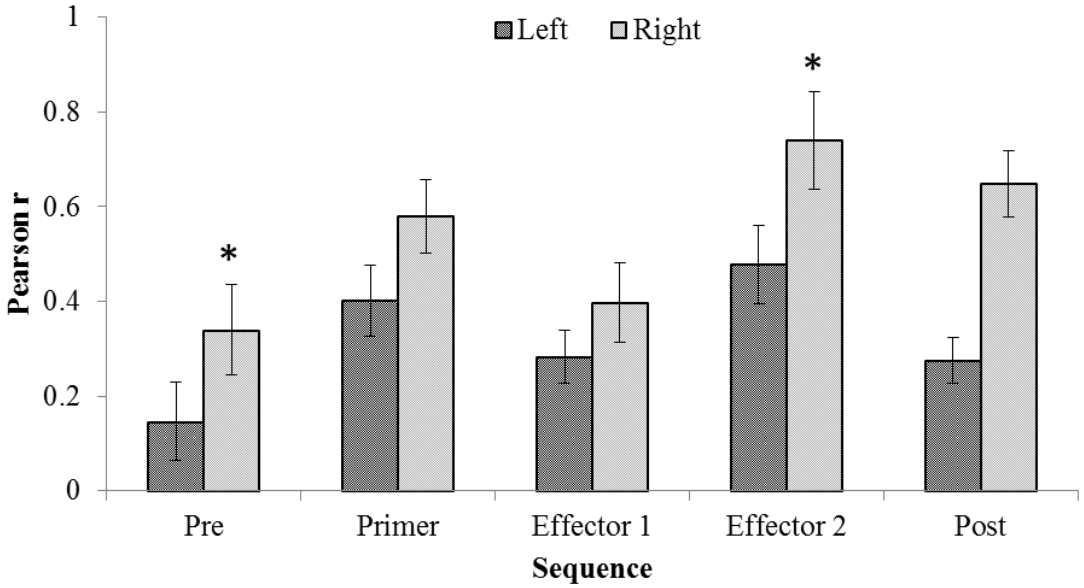

Figure 12. Average correlation coefficient indicative of the strength of the association between global spectral power density for sensors over the left (dark) and right (light) hemispheres for paired individuals.

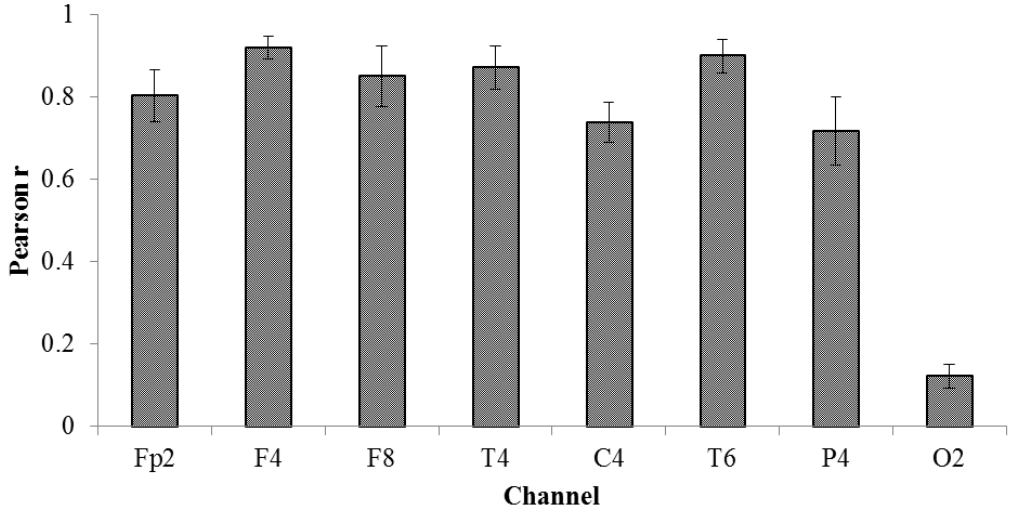

Figure 13. Average correlation coefficients indicative of the strength of the association between global spectral power densities displayed at sensors over the right hemisphere for paired individuals during the second half of the Effector sequence (Effector 2).

Figure 14 shows mean differences between correlation coefficients associated with μV from the left and right hemispheric sensors. These computed values, with their measures of dispersion, are indicative of the magnitude of the global spectral power density coherence disparity between the left and right hemispheres of the paired individuals over the course of the experiment. This was accomplished by subtracting left-hemisphere-associated correlation coefficients from right-hemisphere-associated correlation coefficients. An ANOVA revealed that

this measure differed as a function of the sequence of the experiment, $F(4,21)= 4.83$, $p<.01$, $\eta^2=.53$. The source of the variance associated was an increased value for this metric associated with the Post-Baseline (M= .37, SE= .06) relative to the Effector 1 sequence (M= .11, SE= .03) at the point of inflection, $t(7)= -3.52$, $p=.01$, $r^2= .64$.

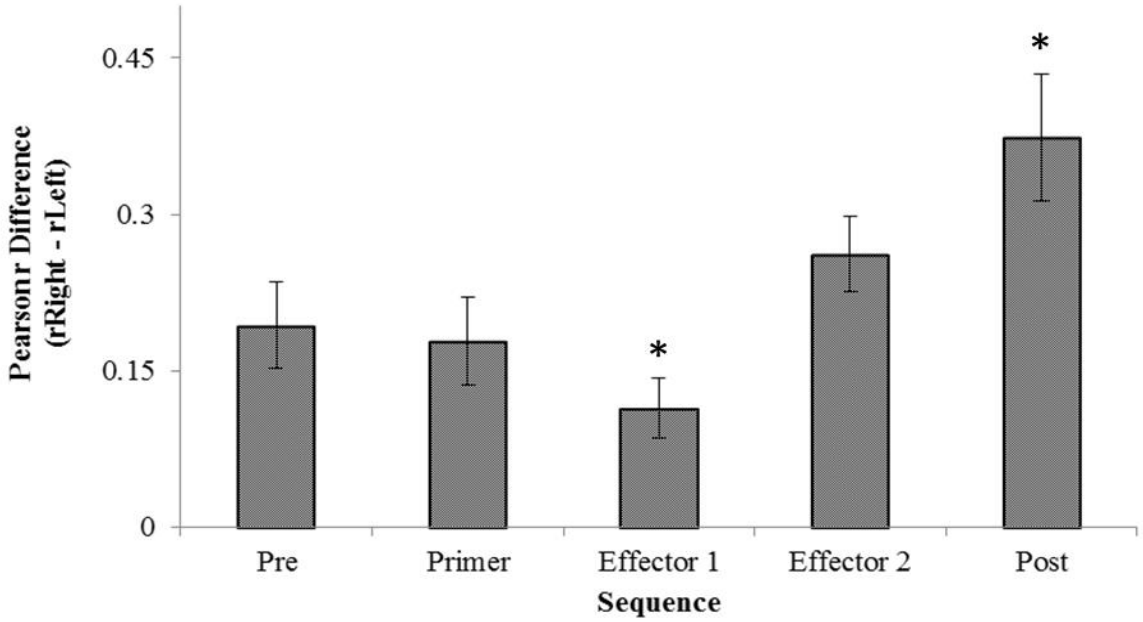

Figure 14. Difference scores obtained by subtracting correlation coefficients indicative of the strength of the association between global power spectral densities for sensors over the left hemisphere of paired individuals from those displayed over the right hemisphere as a function of the sequence of the experiment.

Excess Correlations Between Subjects at a Distance: Intrahemispheric and Interhemispheric Coherence

The mean coherence values for the five pairs of participants over the blocks of the protocol for power within the **theta** and **gamma** bands between the left and right hemisphere for each of the four lobes indicated that the only major significant and obvious effects involved the *temporal* lobes. These bands are the predominant interaction mode between the hippocampal formation and cerebral cortices (Bear, 1996; Whitman et al, 2013). The other frequency bands, delta, alpha-1, alpha-2, beta-1, and beta-2 did not exhibit any significant coherence differences across the phases of the experiment for the shared hemispheric activity for the pairs of participants. The parietal, occipital and frontal regions did not show this effect during the effector field period. There was a marginally significant increase in coherence over the right prefrontal regions for gamma activity during the beginning of the experiment when the instructions were given and individuals were concentrating accordingly.

The conspicuous effect of changed coherence between the more rostral left (T3) and right (T4) temporal lobes as a function of the phase of the experiment and type of magnetic field configuration is shown in Figure 15. During the effector field only there were statistically

significant (as inferred by the absence of overlap of the SEMs) and transient **diminishments** of the coherence of power within the *theta* bands between the *right* temporal lobes of the pairs of individuals separated by ~6000 km. This was not evident for the left temporal region for this frequency band or for the theta band for either temporal lobe.

The specificity of the (right) temporal lobe (and not other lobes) and the gamma band (compared to all other bands) strongly suggests the effect was not simply an artifact of direct exposure to the simultaneously applied toroidal fields. This effect was also not apparent during the primer fields, which also strongly indicates the effect was not due to simply shared magnetic fields. The diminishment was from a right temporal (person 1) to right temporal (person 2) value of 0.15 to 0.10 or a shift of 0.05. For comparison the typical correlations between spike counts from groups of individual neurons in cortical networks range between 0.1 to 0.3 (Ecker et al, 2010).

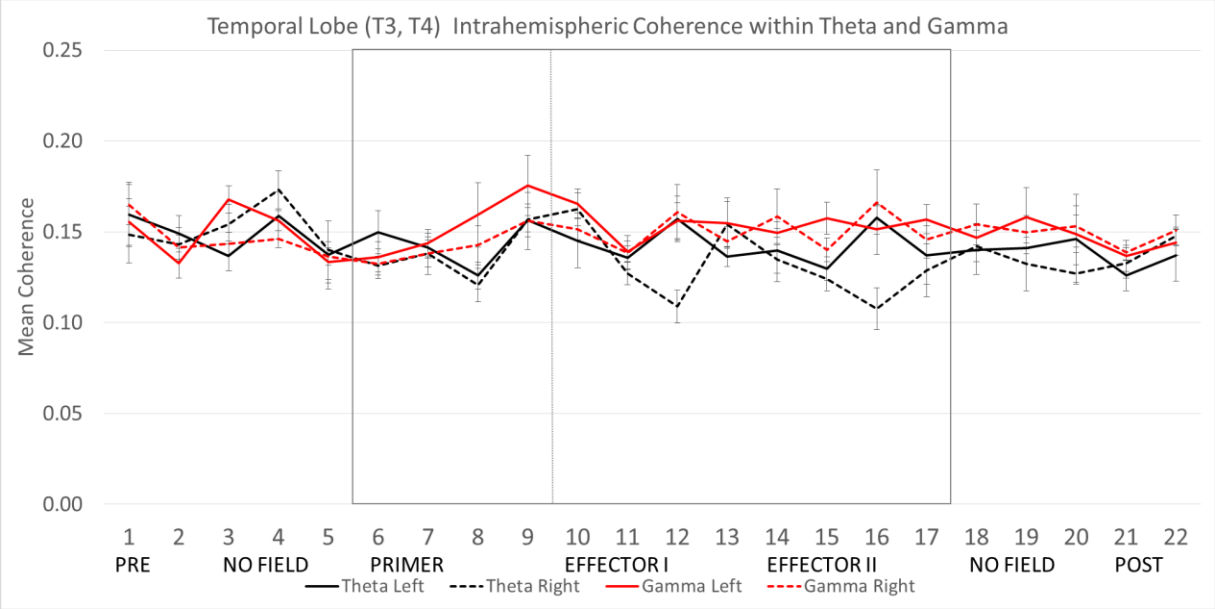

Figure 15. Mean coherence between the left temporal (T3) and right (T4) temporal sensors for the pairs for the theta and gamma band. The only statistically significant differences occurred during the entanglement (effector) stage associated with the depression for right theta coherence. Vertical bars indicate SEMs.

A similar effect was noted only during the effector field condition for the region of the more caudal portion of the temporal lobes (T5, T6). However in this region the diminishment of interbrain coherence during the latter portion of the effector phase occurred for both the left and right hemisphere. It is relevant that these two surface sensor positions are most strongly correlated with activity within the parahippocampal gyrus. The parahippocampal gyrus is the general region by which interactions between the two hippocampuses are mediated through the dorsal hippocampal commissure. It is located in the rostral portion of the splenium of the corpus

callosum. The dorsal hippocampal commissure in the human being mediates information between the hippocampal formations within the left and right hemisphere without processing through the neocortices. Consequently memory modifications can occur without self-awareness.

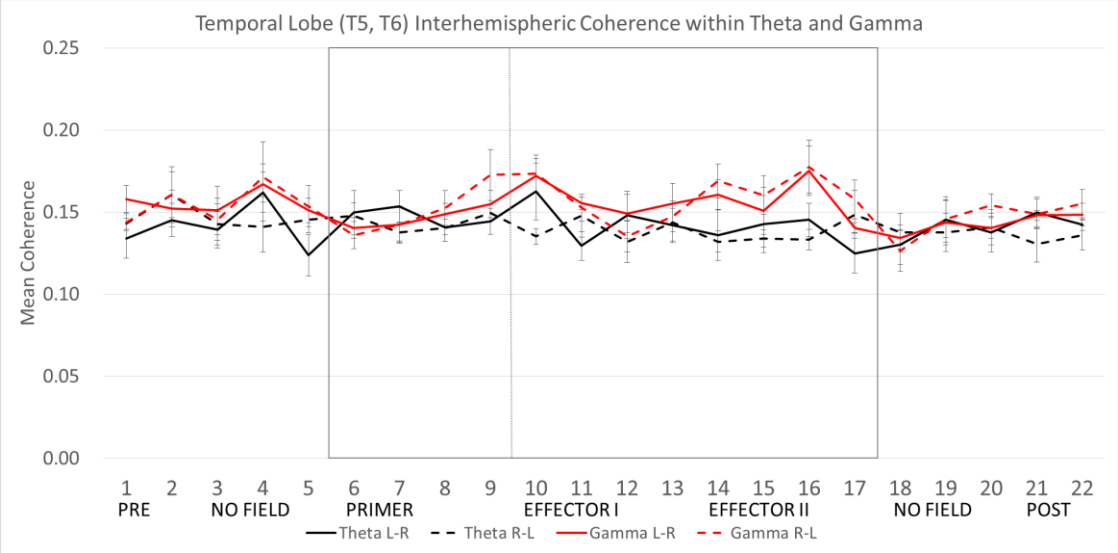

Figure 16. Mean coherence between the left temporal (T5) and right (T6) temporal lobes for each pair (separated by 6000 km) for the power within the gamma and theta band over the various conditions of the experiment. The only statistically significant differences occurred during the entanglement (Effector II) stage. Vertical bars indicate SEMs.

(Continued on Part II)